High-intensity interminiband terahertz emission from chirped superlattices

Cite as: Appl. Phys. Lett. **80**, 1867 (2002); https://doi.org/10.1063/1.1461054
Submitted: 15 November 2001 • Accepted: 16 January 2002 • Published Online: 12 March 2002

Rüdeger Köhler, Alessandro Tredicucci, Fabio Beltram, et al.

High-intensity interminiband terahertz emission from chirped superlattices

Rüdeger Köhler,[a] Alessandro Tredicucci, and Fabio Beltram
NEST–INFM and Scuola Normale Superiore, Piazza dei Cavalieri 7, 56126 Pisa, Italy

Harvey E. Beere, Edmund H. Linfield, A. Giles Davies, and David A. Ritchie
Cavendish Laboratory, University of Cambridge, Madingley Road CB3 0HE, United Kingdom

(Received 15 November 2001; accepted for publication 16 January 2002)

Electroluminescence at $\lambda \sim 69\ \mu$m (4.3 THz) is reported from interminiband transitions in quantum-cascade structures with superlattice active regions. Spontaneous emission gives a low-temperature linewidth of 2 meV (0.48 THz) with linear light–current characteristics observed up to high-current densities ($625\ \mathrm{A/cm^2}$), resulting in record output powers of 500 pW. Devices operate up to above liquid-nitrogen temperature, with both emission wavelength and current–voltage characteristics in good agreement with theoretical predictions. © *2002 American Institute of Physics.* [DOI: 10.1063/1.1461054]

The THz region of the electromagnetic spectrum still lacks compact, coherent, solid-state radiation sources. A promising candidate to fill this gap is the quantum cascade (QC) laser.[1] Quantum cascade lasers (QCLs) are unipolar semiconductor structures in which electrons are fed sequentially from an injector region into the active region (coupled quantum wells or superlattices) and then into the subsequent injector of a repeated epitaxially grown heterostructure. QCLs have shown very high performance in the midinfrared[2,3] and can now be operated at wavelengths as long as 24 μm.[4] This has stimulated a number of studies on QC structures designed for emission at THz frequencies,[5–7] well below the forbidden phonon reststrahlen band. These devices are all based on transitions between subbands in isolated quantum wells and are characterized by low-output powers (typically, a few pW) and low currents, limited by negative differential resistance (NDR) effects. These shortcomings can be largely attributed to poor tunnel coupling of injector states with the active region, and to the choice of narrow injector minibands. The latter is necessary to avoid cross absorption of the emitted light and detrimental nonradiative relaxation through optical-phonon emission. These features seriously hinder efficient extraction of electrons from the lower state of the optical transition. In fact, population inversion has not been observed to date.

In this letter, we report on THz electroluminescence from a QC device based on an alternative structure designed to overcome the problems described above. In this structure, radiative emission takes place across the first minigap of a graded superlattice (SL), which allows large interminiband dipole matrix elements (7.8 nm, in this case) without requiring high dopant concentrations to avoid field-induced localization.[8] To minimize electron population in the lower state of the transition, we engineered the first SL miniband to comprise seven subbands spanning an energy of 17 meV. This energy is slightly less than that of the photon, in order to avoid cross absorption, and provides a large phase space into which electrons scattered from the upper miniband or directly from the injector can spread. In addition, the wide miniband dispersion allows for high operating currents and suppresses thermal backfilling. Details of the design can be found in Ref. 9, where Monte Carlo simulations, including both carrier–carrier and carrier–phonon scattering, showed that such a structure is indeed capable of carrying much higher current densities, and, owing to the improved injection/extraction into/out of the active region, can exhibit population inversion. The active core of our sample consists of 40 $Al_{0.15}Ga_{0.85}As$/GaAs SL-injector stages (see the inset of Fig. 1 for a schematic band diagram). Starting from the injection barrier the layer sequence of each period reads ***4.3***/18.8/***0.8***/15.8/***0.6***/11.7/***2.5***/10.3/**2.9**/10.2/**3.0**/10.8/**3.3**/9.9. Thickness values are given in nm with barriers in bold face, and italics identifying the SL. The 10.2-nm-wide GaAs well is n doped to $4\times10^{16}\ \mathrm{cm^{-3}}$. This active core is sandwiched between a highly doped ($n=2\times10^{18}\ \mathrm{cm^{-3}}$) GaAs upper contact layer of thickness 200 nm and a 500 nm GaAs buffer layer ($n=2\times10^{18}\ \mathrm{cm^{-3}}$).[9] The entire stack was grown by

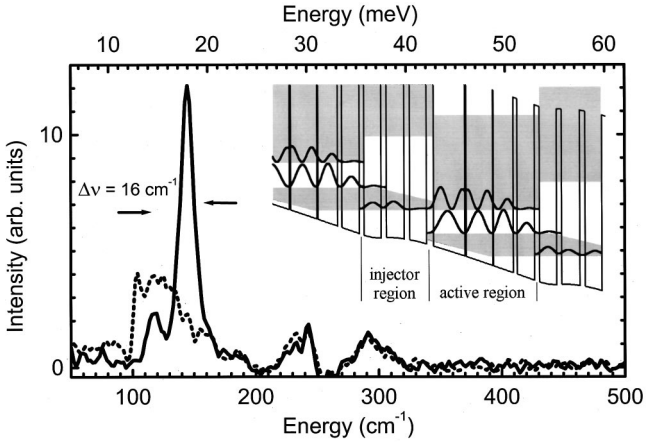

FIG. 1. Electroluminescence spectra recorded at 8 K. The solid line is taken in forward bias at a current of 1000 mA and with a pulse length of 800 ns (20% overall duty cycle). The dotted line is the reverse bias spectrum at an equal dissipated power. The main peak at $144\ \mathrm{cm^{-1}}$ is attributed to the intersubband transition and is absent in the reverse bias spectrum, as expected from the asymmetry of the structure. Inset: schematic diagram of the conduction band in the active core. The moduli squared of the wave functions involved in the optical transition are shown; shaded areas represent the SL minibands. See Ref. 9 for a complete discussion.

[a]Electronic mail: koehler@nest.sns.it

molecular-beam epitaxy on a n^+-GaAs substrate. The samples were then processed into square mesas of 400 μm side by optical contact lithography and wet-chemical etching. The wafers were thinned down to about 250 μm in order to improve heat dissipation, and Ohmic Ge/Au contacts were provided to the top and back surfaces of the sample by thermal evaporation and subsequent annealing under a nitrogen atmosphere. The top contact simultaneously served as a grating coupler in order to diffract the in-plane emitted light out of the sample. Grating periods of 15, 18, 21, and 24 μm were used. The devices were finally soldered with an In–Ag alloy onto a copper block and mounted on the cold finger of a liquid-He flow cryostat equipped with polyethylene windows. To reduce heating effects, trains of 750 current pulses (width ranging from 600 to 1400 ns, period of 2 μs) were applied to the device, with a train repetition rate of 333 Hz, chosen to match the frequency response of the detector. THz radiation was collected orthogonal to the mesa by a f/1 off-axis parabolic mirror, sent through a Fourier transform interferometer (FTIR), and focused again onto a liquid-He-cooled Si bolometer. The entire beam path was purged with purified air in order to minimize water-vapor absorption. Spectral measurements were performed using the FTIR in step-scan mode and employing a lock-in amplifier for signal detection.

Figure 1 shows two electroluminescence spectra recorded at 8 K heat-sink temperature with a resolution of 4 cm^{-1} from a mesa with an 18-μm-period grating. The solid line corresponds to a spectrum taken with the correct bias polarity, applying 800-ns-long negative pulses of 1000 mA amplitude to the top contact. The dotted line is a spectrum obtained at the same level of dissipated power but under reverse bias. The first spectrum consists of four peaks, with the two peaks at 243 and 292 cm^{-1} corresponding to the GaAs phonon reststrahlen band. The main peak at 144 cm^{-1} (equal to 18 meV) can be unambiguously attributed to the intersubband transition. As expected, it is absent in the spectrum taken under reverse bias. In fact, owing to the asymmetry of the level structure, intersubband emission can only be recorded when the active-region field has the appropriate polarity. This is not the case for other spurious processes such as blackbody emission or impurity-related transitions. Moreover, we performed measurements on mesas with different grating periods ranging from 15 to 24 μm and found this peak present in all spectra. Its intensity, however, decreases with longer grating periods, whereas the 15 μm grating gives almost as good results as the 18 μm grating. This is in good agreement with theoretical predictions[10] and results of previous experiments.[11] Both confirm that the coupling efficiency between the grating and the light is maximum for a grating period slightly shorter than the wavelength, decreasing rapidly towards longer periods and slowly towards shorter periods. The transition energy of 18 meV is in very good agreement with the value calculated from a Schrödinger–Poisson framework at this applied field. At low temperature, the full width at half maximum (FWHM) is 2 meV, which is a little broader than that measured in samples employing a vertical transition within a single quantum well.[5,7] It is well known, however, that SL active regions tend to exhibit broader luminescence peaks since the wave functions involved extend across several barriers and thus are more sensitive to interface roughness. No appreciable increase of the linewidth with drive current amplitude or duty cycle is observed, indicating no significant influence of electron heating effects. The nature of the fourth peak observed at 112 cm^{-1} (11.1 meV) is unclear. This peak is present in various other structures from which we do not detect intersubband emission, and it exhibits linear light–current characteristics. Possible explanations could include shallow donor transitions, or defects located in the interdiffused layer between the GaAs and the Ge–Au top contact. It might also be an artifact of blackbody radiation convoluted with the grating and apparatus response.

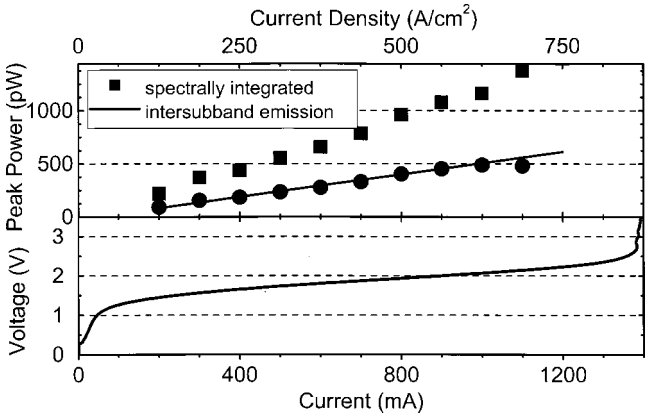

FIG. 2. (a) Light–current and (b) voltage–current characteristics as recorded in pulsed mode (800-ns-long pulses) at 8 K. The values of peak output power were corrected for the absorption of the polyethylene window of the cryostat (see Ref. 12). Squares correspond to the emission spectrally integrated over the whole range (50–600 cm^{-1}), whereas circles represent the power of the intersubband emission peak alone. The solid line is a linear fit to the data from 200 to 1000 mA.

Figure 2 shows the current–light (L–I) and the current–voltage (V–I) characteristics of the device. The upper data (squares) correspond to the spectrally integrated power from 50 to 600 cm^{-1}, whereas the lower data (circles) correspond to the power emitted within the intersubband peak. The latter increases monotonically with current up to 1000 mA (625 $\mathrm{A/cm}^2$), where the highest peak output power of 500 pW was measured.[12] The current–voltage characteristics shown in Fig. 2(b) are typical for transport through QC structures. At low voltages the resistance of the sample is high owing to level misalignment. At a voltage of about 1.1 V, corresponding to an electric field of 3 kV/cm (close to the design field of 3.5 kV/cm), the levels become aligned and injection into the upper SL miniband takes place, as indicated by the differential resistivity dropping to 0.7 Ω. Linear V–I characteristics are obtained over a wide range of currents (from about 400 to 1100 mA), confirming that the large dispersion of the SL miniband ensures efficient electron transport through the structure. At a current of 1300 mA ($\sim$820 $\mathrm{A/cm}^2$) NDR occurs, marking the suppression of resonant tunneling transport. The intersubband emission dependence on the current density is practically linear almost up to the roll-off point. This suggests that the radiative efficiency is not reduced by density-dependent mechanisms like electron–electron or Auger scattering, contrary to previous experiments where a square-root dependence of the emitted light with current was found.[5] In our structure, and in line with theoretical predictions,[9] the linear dependence is better

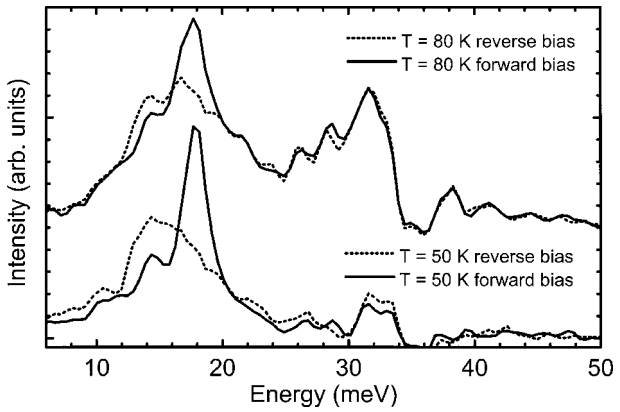

FIG. 3. Spontaneous emission spectra collected at heat-sink temperatures of 50 K (lower curves) and 80 K (upper curves) at an injection current of 800 mA using 1-μs-long pulses. The spectra at 80 K are offset for clarity. The forward bias spectra are plotted as solid lines, while reverse bias ones are dotted. The intersubband emission is clearly detectable up to 80 K, however, its intensity decreases significantly with temperature and the linewidth becomes considerably broader.

explained by activated carrier-phonon scattering with a small activation energy. At the current density of 625 A/cm^2, where we observe the maximum output power, the carrier density in the upper state can be estimated to be 3.1×10^9 cm^{-2} from the calculated level lifetime.[9] The expected optical output power of 260 nW can then be derived from the number of periods, the photon energy, and the transition dipole moment.[5] This is approximately three orders of magnitude higher than the measured value of 500 pW, which is quite reasonable taking into account the grating coupling efficiency and the collection efficiency of our apparatus. The $L-I$ roll off at higher currents can be attributed to the onset of misalignment between the injector ground state and the upper level of the optical transition owing to the increasing bias voltage. Such misalignment causes poorer injection efficiency and thereby reduces the optical output power.

Figure 3 shows the luminescence spectra obtained at heat-sink temperatures of (a) 50 K and (b) 80 K for a drive current of 800 mA. Intersubband emission is clearly visible up to 80 K, although the intensity decreases significantly with increasing temperature. For comparison, we also plot the spectra recorded in reverse bias together with the 8 K spectrum. The emission slightly shifts towards longer wavelengths and broadens with increasing temperature, which is in line with the behavior observed in midinfrared QC lasers.

In summary, far-infrared (THz) electroluminescence from a quantum cascade device with superlattice active regions has been investigated. Unlike previous structures[5,7] where sublinear light–current characteristics were observed, our sample exhibits a linear response up to a current density of 625 A/cm^2. The measured peak output power at this current is about a factor of 10 higher than values previously reported in the literature. This can be explained by the improved transport characteristics of the structure and the large dipole matrix element of the superlattice active region.

This work was supported in part by the European Commission through an IST Framework V FET project WANTED. One of the authors (R.K.) acknowledges support by the C.N.R.; two of the authors (E.H.L. and A.G.D.) acknowledge support from Toshiba Research Europe Ltd. and the Royal Society, respectively. The authors thank Sukhdeep Dhillon for helpful discussions.

[1] J. Faist, F. Capasso, D. L. Sivco, C. Sirtori, A. L. Hutchinson, and A. Y. Cho, Science **264**, 553 (1994).
[2] D. Hofstaetter, M. Beck, T. Aellen, J. Faist, U. Oesterle, M. Illegems, E. Gini, and H. Melchior, Appl. Phys. Lett. **78**, 1964 (2001).
[3] R. Paiella, R. Martini, F. Capasso, C. Gmachl, H. Y. Hwang, D. L. Sivco, J. N. Baillargeon, A. Y. Cho, E. A. Whittaker, and H. C. Liu, Appl. Phys. Lett. **79**, 2526 (2001).
[4] R. Colombelli, F. Capasso, C. Gmachl, A. L. Hutchinson, D. L. Sivco, A. Tredicucci, M. C. Wanke, A. M. Sergent, and A. Y. Cho, Appl. Phys. Lett. **78**, 2620 (2001).
[5] M. Rochat, J. Faist, M. Beck, U. Oesterle, and M. Ilegems, Appl. Phys. Lett. **73**, 3724 (1998).
[6] B. S. Williams, B. Xu, Q. Hu, and M. R. Melloch, Appl. Phys. Lett. **75**, 2927 (1999).
[7] J. Ulrich, R. Zobl, K. Unterrainer, G. Strasser, and E. Gornik, Appl. Phys. Lett. **76**, 19 (2000).
[8] A. Tredicucci, F. Capasso, C. Gmachl, D. L. Sivco, A. L. Hutchinson, and A. Y. Cho, Appl. Phys. Lett. **73**, 2101 (1998).
[9] R. Köhler, R. C. Iotti, A. Tredicucci, and F. Rossi, Appl. Phys. Lett. **79**, 3920 (2001).
[10] B. Xu and Q. Hu, Appl. Phys. Lett. **70**, 2511 (1997).
[11] M. Helm, E. Colas, P. England, F. DeRosa, and S. J. Allen, Jr., Appl. Phys. Lett. **53**, 1714 (1988).
[12] The optical output power was calculated using the responsitivity of the bolometer as calibrated against blackbody radiation by the manufacturer (QMC Instruments). The transmission of the polyethylene window was measured to be 0.62 at the wavelength of interest.